Journal of Magnetic Resonance 208 (2011) 225–234

Contents lists available at ScienceDirect

Journal of Magnetic Resonance

journal homepage: www.elsevier.com/locate/jmr

Double-quantum homonuclear correlations of spin $I = 5/2$ nuclei

Dinu Iuga *

Physics Department, University of Warwick, CV4 7AL Coventry, UK

ARTICLE INFO

Article history:
Received 10 June 2010
Revised 3 November 2010
Available online 16 November 2010

Keywords:
Half-integer quadrupolar nuclei
Homonuclear correlations
Gamma alumina

ABSTRACT

The challenges associated with acquiring double-quantum homonuclear Nuclear Magnetic Resonance correlation spectra of half-integer quadrupolar nuclei are described. In these experiments the radio-frequency irradiation amplitude is necessarily weak in order to selectively excite the central transition. In this limit only one out of the 25 double-quantum coherences possible for two coupled spin $I = 5/2$ nuclei is excited. An investigation of all the 25 two spins double quantum transitions reveals interesting effects such as a compensation of the first-order quadrupolar interaction between the two single quantum transitions involved in the double quantum coherence. In this paper a full numerical study of a hypothetical two spin $I = 5/2$ system is used to show what happens when the RF amplitude during recoupling is increased. In principle this is advantageous, since the required double quantum coherence should build up faster, but in practice it also induces adiabatic passage transfer of population and coherence which impedes any build up. Finally an optimized rotary resonance recoupling (oR^3) sequence is introduced in order to decrease these transfers. This sequence consists of a spin locking irradiation whose amplitude is reduced four times during one rotor period, and allows higher RF powers to be used during recoupling. The sequence is used to measure ^{27}Al DQ dipolar correlation spectra of $Y_3Al_5O_{12}$ (YAG) and gamma alumina (γAl_2O_3). The results prove that aluminium vacancies in gamma alumina mainly occur in the tetrahedral sites.

1. Introduction

Nuclear Magnetic Resonance (NMR) experiments on solid samples containing half-integer quadrupolar nuclei result in similar structural information to those designed for spin-1/2 nuclei. The central transition (CT) of a half-integer quadrupolar nucleus is not broadened to first-order by the quadrupolar interaction. Magic angle spinning (MAS) removes part of the residual second-order quadrupolar broadening, so that NMR spectra can resolve chemically different sites in order to find answers to structural questions. Furthermore, two-dimensional experiments like MQMAS [1] and STMAS [2] can remove the second-order quadrupolar broadening, providing high resolution NMR spectra of half-integer quadrupolar nuclei. These experiments are now widely accepted and routinely used for structural investigation of materials, such as zeolites, ceramics and biomaterials [3,4].

MAS averages the large dipolar interactions observed for solid samples, resulting in high resolution spectra. However, the dipolar interaction contains important structural information, such as internuclear distances, and in order to retrieve this, the dipolar interaction must be reintroduced in a controlled fashion. For spins-1/2 many experiments have been introduced [5 and references therein]. However, if one of the dipolar-coupled nuclei is quadrupolar, MAS cannot completely remove the dipolar interaction because the dipolar Hamiltonian does not commute with the quadrupolar Hamiltonian. This means that a quadrupolar-driven recoupling of the homo and/or heteronuclear dipolar interaction occurs during MAS experiments. These "residual" dipolar couplings were reported in 1980 [6] and analyzed by Menger [7]. Therefore, it might be expected that dipolar correlation spectra could be obtained without the need for a recoupling sequence. However, this approach is complicated by the fact that quadrupolar nuclei usually suffer from rapid loss of coherence and there is insufficient time for evolution under the residual dipolar coupling to generate a double quantum (DQ) coherence. Therefore, recoupling sequences designed to operate with quadrupolar nuclei are required [8], but the development of such recoupling sequences is difficult because the quadrupolar interaction is very large compared with the dipolar interaction and quadrupolar nuclei have more than two energy levels rendering the dynamics of the spin system much more complicated.

Two interactions can be used for creating homo and heteronuclear correlations: the through-space and through-bond (J-coupling) dipolar interactions. This paper is mostly concerned with the through-space dipolar interaction, but two-dimensional scalar correlation experiments operating via J-coupling between a half-integer quadrupolar nucleus and a spin-1/2 nucleus have been demonstrated [9]. In addition, heteronuclear correlations obtained through J-coupling between two quadrupolar nuclei (^{27}Al and ^{17}O)

* Fax: +44 (0) 24 76150897.
E-mail address: d.iuga@warwick.ac.uk

1090-7807/$ - see front matter © 2010 Elsevier Inc. All rights reserved.
doi:10.1016/j.jmr.2010.11.007

have been reported [10]. The J-coupling does not vanish during MAS, but long mixing times are required to develop two spin coherences, and therefore this approach can only be used for spins that have a long T_2' relaxation time. In order to increase the T_2' of quadrupolar nuclei spin the sample can be spun slightly off the magic angle [11]. In this case the spinning sidebands of the satellite transitions do not overlap with the CT and therefore rotational resonance between the CT and the satellite transitions is reduced, increasing the T_2'.

Homonuclear correlations based on the through-space dipolar interaction can be further split into two categories; experiments that produce SQ–SQ correlations and experiments that produce DQ–SQ correlations. The first category includes homonuclear correlations using rotary resonance (HORROR) adapted for half-integer quadrupolar nuclei [12]; spinning away from the magic angle [13]; spin diffusion under double angle rotation [14]; rotary resonance recoupling [15] and symmetry-based recoupling sequences [16]. DQ–SQ homonuclear correlations between quadrupolar nuclei have been demonstrated using rotary resonance recoupling (R^3) [17] or symmetry-based recoupling sequences [18–20].

This paper is concerned with the second category, namely experiments that produce DQ–SQ homonuclear correlations. For this category, and in general when working with quadrupolar nuclei, very weak RF pulses that are selective to the CT are usually employed in order to avoid leakages of coherence due to adiabatic passages [21]. For this reason in order to match the $\omega_{MAS}/2$ or ω_{MAS} rotary resonance condition [22,23] for weak RF irradiation the spinning speed must also be low. This condition severely limits the applicability of this experiment to real systems containing half-integer quadrupolar nuclei, which require rapid MAS due to the large quadrupolar interaction. In addition, using weak RF irradiation to create the DQ coherence imposes longer DQ excitation and conversion times. In such a case one must be aware of the difficulties of spin locking the central transition of half-integer quadrupolar nuclei. During sample spinning, RF irradiation of the quadrupolar spin system induces adiabatic passage transfers that scramble the spin populations and spin coherences. The scrambling effect depends on the orientation and therefore the free induction decay dephases rapidly. An understanding of the phenomena occurring during spin locking [24] is essential for designing DQ–SQ correlations experiments for quadrupolar nuclei.

This paper analyzes a theoretical spin system formed by two dipolar-coupled $I = 5/2$ spins. In such a spin system there are 36 energy levels and 25 DQ transitions. We demonstrate that cancellation of the first-order quadrupolar interaction occurs for several DQ transitions. This cancellation can be complete for identical spins, so that in this case the DQ transitions are not affected by the first-order quadrupolar interaction. The paper further investigates the phenomena that occur while irradiating a quadrupolar spin system and describes what happens when the RF irradiation is not sufficiently low to avoid adiabatic passage transfers. An understanding of these phenomena is essential for avoiding excitations of unwanted DQ coherences that cancel the desired |1/2, 1/2 > |−1/2, −1/2 > DQ coherence. A new pulse sequence that allows for stronger RF irradiation, while reducing the negative effect of adiabatic passage transfers for some of the orientations is introduced. The sequence consists in irradiation at rotary resonance condition with amplitude that is reduced for four short time periods per rotor period. The new sequence allowed us to obtain ^{27}Al homonuclear correlation spectra of YAG and of γAl_2O_3.

2. Double quantum coherences

When two spin $I = 5/2$ nuclei are coupled through a dipolar coupling a spin system with 36 energy levels is formed. In a powder sample the quadrupolar interactions of the two spins broaden the energy levels. Fig. 1 shows the energy level diagram for an hypothetical spin system formed by two identical spin $I = 5/2$ nuclei. A quick analysis of the figure indicates that different levels are broadened by a different amount due to the first-order quadrupolar interaction. For example the level $|I_1 = 5/2, I_2 = 5/2>$ will be broaden by the sum of the two quadrupolar interactions, whereas for the level |−1/2, 5/2> the first-order quadrupolar interactions will cancel each other.

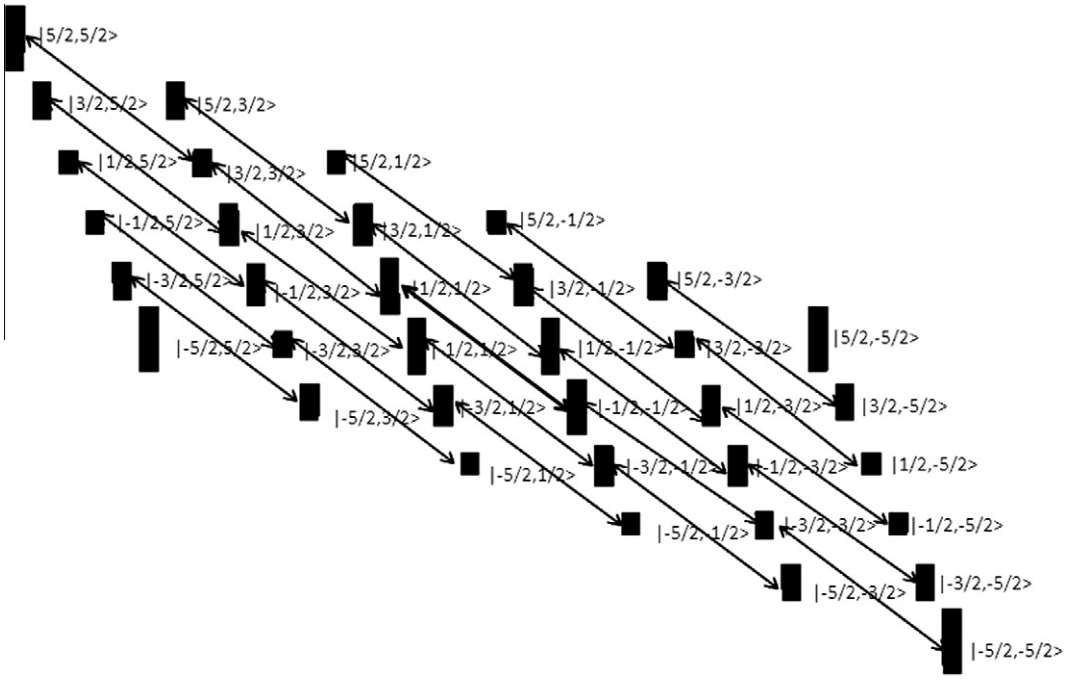

Fig. 1. Energy level diagram of two spin $I = 5/2$ nuclei coupled. The ratio between quadrupolar interaction and Zeeman interaction was artificially increased. The width of the levels indicates whether quadrupolar interaction of the energy involved compensates or adds up. A level is represented as |1, 2>, where |1> refers to the eigenvalue of the quantum moment of the first spin and 12> is the eigenvalue of the quantum moment of the second spin. The 25 DQ transitions are indicated with arrows.

A two-spin DQ transition occurs when both spins undergo a single quantum transition in the same direction whereas a two-spin zero-quantum (ZQ) transition occur when the two spins involved follow a transition in the opposite direction. For example a transition from |5/2, 5/2> to |3/2, 3/2> is a DQ transition whereas a transition between |1/2, 5/2> and |3/2, 3/2> is a ZQ transition. In a spin system formed by two coupled $I = 5/2$ spins, there are 25 two-spin DQ transitions (shown on Fig. 1) and 25 ZQ transitions (not shown). The two-spin DQ transitions bear information concerning the coupling between the two spins and therefore an

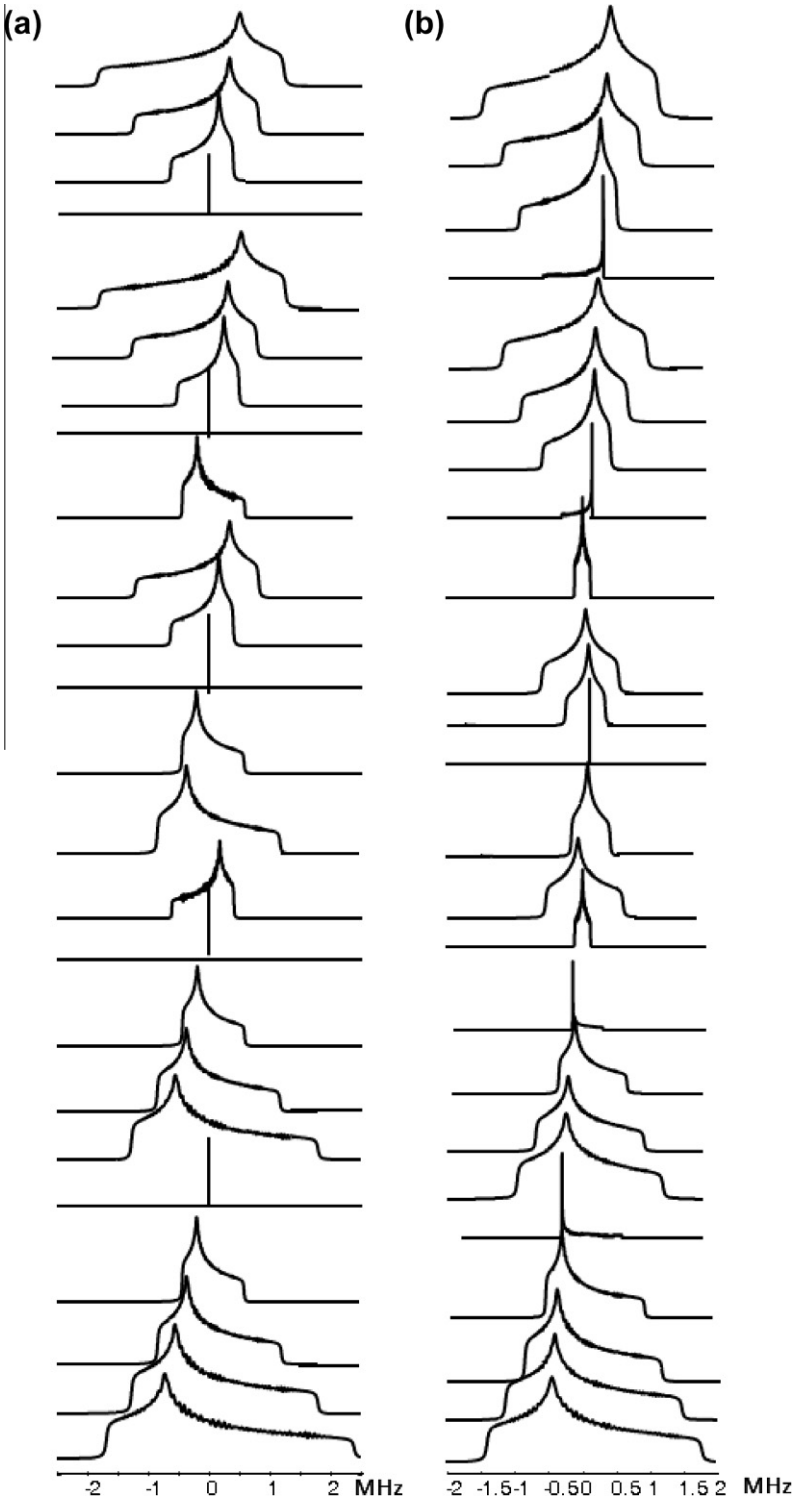

Fig. 2. Static first-order quadrupolar broadening of a double quantum transition for (a) identical spin $I = 5/2$ nuclei ($C_{qcc} = 4$ MHz $\eta = 0.4$) and (b) non-identical spin $I = 5/2$ nuclei ($C_{qcc1} = 4$ MHz $\eta_1 = 0.4$; $C_{qcc2} = 2$ MHz $\eta_2 = 0.8$, relative orientation between the spins ($\alpha = 30°$, $\beta = 45°$, $\gamma = 0°$). From top to bottom the DQ transitions are: (|−3/2, −3/2> to |−5/2, −5/2> C1); (|−3/2, −1/2> to |−5/2, −3/2> C2); (|−3/2, 1/2> to |−5/2, −1/2> C3); (|−3/2, 3/2> to |−5/2, 1/2 > C4); (|−3/2, 5/2> to |−5/2, 3/2> C5); (|−1/2, −3/2> to |−3/2, −5/2> C6); (|−1/2, −1/2> to |−3/2, −3/2> C7); (|−1/2, 1/2> to |−3/2, −1/2> C8); (|−1/2, 3/2> to |−3/2, 1/2> C9); (|−1/2, 5/2> to |−3/2, 3/2> C10); (|1/2, −3/2> to |−1/2, −5/2> C11); (|1/2, −1/2> to |−1/2, −3/2> C12); (|1/2, 1/2> to |−1/2, −1/2> C13); (|1/2, 3/2> to |−1/2, 1/2> C14); (|1/2, 5/2> to |−1/2, 3/2> C15); (|3/2, −3/2> to |1/2, −5/2> C16); (|3/2, −1/2> to |1/2, −3/2> C17); (|3/2, 1/2> to |1/2, −1/2> C18); (|3/2, 3/2> to |1/2, 1/2> C19); (|3/2, 5/2> to |1/2, 3/2> C20); (|5/2, −3/2> to |3/2, −5/2> C21); (|5/2, −1/2> to |3/2, −3/2> C22); (|5/2, 1/2> to |3/2, −1/2> C23); (|5/2, 3/2> to |3/2, 1/2> C24); (|5/2, 5/2> to |3/2, 3/2> C25);

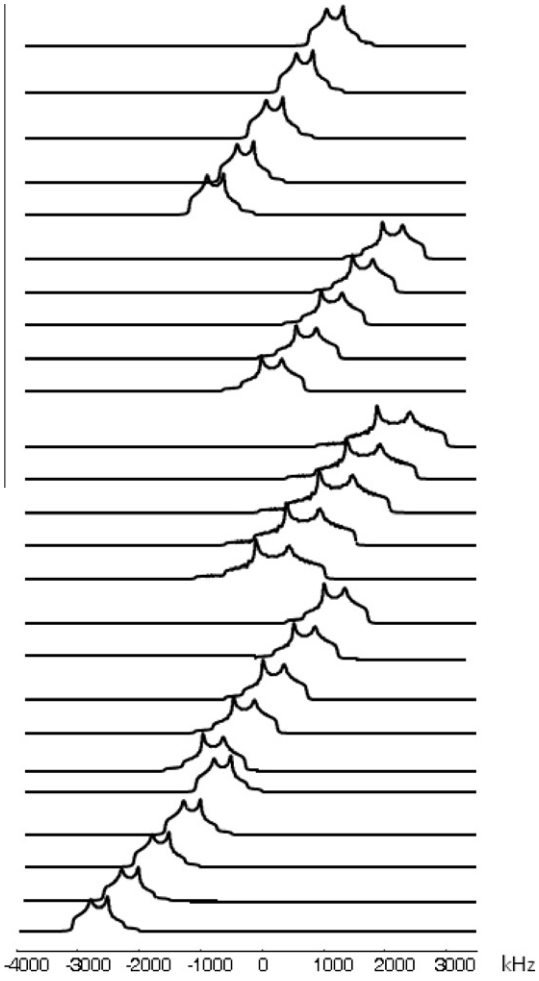

Fig. 3. Second order lineshape for the 25 DQ transitions. Two identical spin $I = 5/2$ nuclei ($C_{qcc} = 4$ MHz $\eta = 0.4$ $\nu_L = 130$ MHz) were considered. From top to bottom the DQ coherences are from C1 to C25.

NMR experiment that detects the DQ coherence will reveal the homonuclear correlations present in the sample.

For further insight into the DQ transitions it is useful to compare them with the SQ transitions for a single spin $I = 5/2$. A spin $I = 5/2$ nucleus has a central transition between |1/2> and |−1/2> levels, not affected by the first-order quadrupolar interaction and other SQ satellite transitions (|5/2> → |3/2>; |3/2> → |1/2>; |−1/2> → |−3/2>; |−3/2> → |−5/2>) broadened by the first-order quadrupolar interaction. For $C_{qcc} = 4$ MHz and $\eta = 0.4$ in a powder sample, where all the orientations of the quadrupolar tensor with respect to the external magnetic field are possible, the transitions between |±3/2> and |±5/2> are spread over a 2.4 MHz, whereas the transitions between |±1/2> and |±3/2> are 1.2 MHz wide. In MAS experiments these transitions result in spinning sidebands. Now making a similar investigation of the DQ transitions in a spin system formed by two coupled spin $I = 5/2$ nuclei, we obtain the static first-order quadrupolar line shape of the 25 DQ transitions shown in Fig. 2. For the transitions |5/2, 5/2>|3/2, 3/2> and |−3/2, −3/2>|−5/2, −5/2> the first-order quadrupolar interactions of the two spins add resulting in broader transitions, whereas for the transitions |5/2, −3/2>|3/2, −5/2>; |3/2, −1/2>|1/2, −3/2>; |1/2, 1/2>|−1/2, −1/2>; |−1/2, 3/2>|−3/2, 1/2> and |−3/2, 5/2>|−5/2, 3/2> the first-order quadrupolar interaction cancels. Therefore the former five transitions are not affected to first order. This observation is very interesting and may lead to other solutions for DQ–SQ correlation experiments. If the spins are not identical, i.e. they have different quadrupolar interactions with different quadrupole coupling constant, asymmetry and orientation, for some of the DQ transitions there still exists a significant compensation between the quadrupolar interactions of the two spins leading to reduced quadrupolar broadening. This indicates a second important observation namely that identical homonuclear spin pairs behave differently to non-identical homonuclear spin pairs. At this point it is useful to raise the question: Is the RF irradiation creating the DQ transitions from SQ transitions or directly from equilibrium populations?, if the former, then the quadrupolar broadening of a SQ coherence can be refocused by another SQ coherence with the opposite quadrupolar broadening.

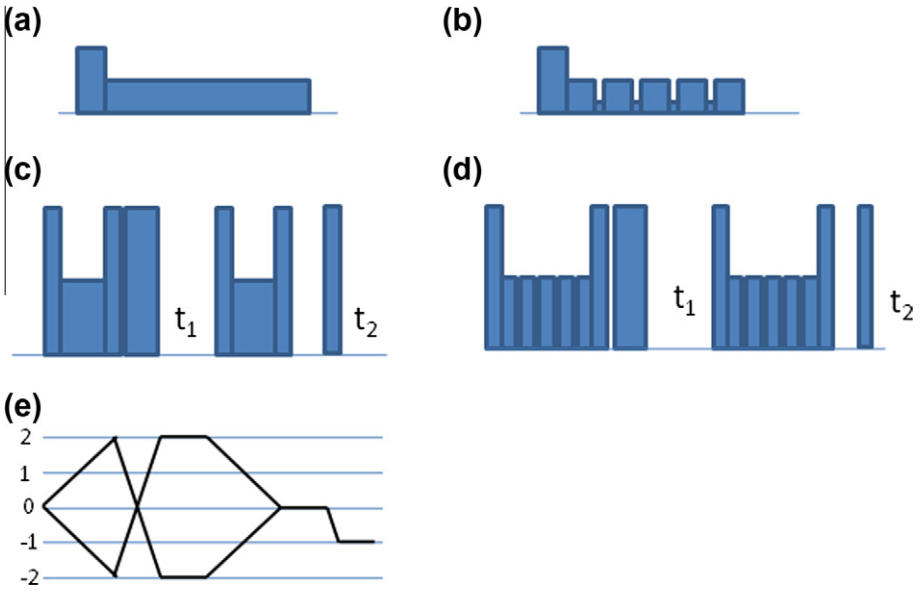

Fig. 4. Pulse sequences used in this study. (a) Spin locking, (b) spin locking using an oR^3 sequence, (c) pulse sequence for measuring DQ–SQ homonuclear correlations using R^3 sequence, (d) pulse sequence for measuring DQ–SQ homonuclear correlations using oR^3 sequence. A phase cycle that selects the coherence transfer pathway shown in and (e) was used for the DQ–SQ homonuclear correlation experiments.

Closer examination of the spinning sidebands which result from the first-order quadrupolar broadening reveal a powder lineshape explained by a second order perturbation treatment of the quadrupolar interaction. This second order broadening affects all the SQ transitions of a spin $I = 5/2$ nucleus and will therefore affect all two-spin DQ transitions of two coupled spin $I = 5/2$ nuclei. Fig. 3 shows the effect of the second-order quadrupolar interaction on the 25 DQ transitions under MAS. The positions of the lines vary, since the quadrupolar induced shifts are different for different transitions. The 25 DQ transitions cannot be separated from one another by phase-cycling procedures. Therefore, the DQ dimension of a DQ–SQ correlation spectrum will contain not only a DQ coherence from the $|-1/2, -1/2\rangle|1/2, 1/2\rangle$ transition, but all possible DQ transitions. When all the 25 lineshapes shown in Fig. 3 overlap a very broad, non-interpretable spectrum will result.

Therefore, it is important to establish the DQ excitation efficiency for the individual coherences, since this determines the overall sensitivity of the experiment and the lineshape in the DQ dimension. Of course this depends additionally on the excitation and reconversion schemes chosen, but here we analyze the excitation produced by a rotary resonance condition used previously [17]. This excitation sequence, displayed in Fig. 4a, consists of a soft 90° pulse followed by a soft spin lock pulse of duration equal to an integral number of rotor periods. Fig. 5 shows the excitation profile of all 25 DQ coherences for three values of the spin lock RF amplitude. The figure highlights the requirement that the pulses are selective for the central transition, since otherwise other DQ transitions are excited leading to line broadening and reduced intensity in the DQ spectrum. More importantly one can see that while some coherences have positive intensities others are negative, so that cancellation of the desired signal occurs.

Further insight into how the DQ coherences are created can be gained by an investigation of the adiabatic passages which occur during the experiment. In MAS experiments each spin feels a quadrupolar interaction that oscillates, so that during a rotor period there are several zero crossings when the quadrupolar interaction changes sign. These zero crossings induce adiabatic transfers between energy levels population and coherences. Fig. 6a shows the behaviour of the quadrupolar interaction of a spin $I = 5/2$ nucleus (with orientation $\alpha = 156°$ $\beta = 98°$ $\gamma = 12°$) during one rotor period. The transfers of populations between the energy levels with RF irradiation at 5 kHz and 50 kHz are shown in Fig. 6c and e. One can clearly see that a 5 kHz irradiation is selective to central transition, whereas during a 50 kHz irradiation all the populations are scrambled. Similar behaviour is expected for a system formed by two coupled spin $I = 5/2$ nuclei. The oscillations of the energy levels over a rotor period are shown in Fig. 6b and the behaviour of the populations during irradiation with a 5 kHz and a 50 kHz RF field is shown in Fig. 6d and f. In this case a 5 kHz irradiation is mostly affecting the $m = \pm 1/2$ energy levels whereas a 50 kHz irradiation affects the populations of all the energy levels. It is this phenomenon of adiabatic passage transfer that allows all 25 DQ coherences to be created regardless of the magnitude of the quadrupolar interaction. The only way to avoid the unwanted coherences and restrict the experiment to the central $|1/2, 1/2\rangle|-1/2, -1/2\rangle$ DQ transition is to use a very low amplitude RF field. Looking at Fig. 6c and e we can say that if the population of the $|3/2\rangle$ energy level changes much during one rotor period, it means that unwanted coherences are more likely to be created whereas if the change in the population of the $|3/2\rangle$ energy level is small, the central transition coherence initially created will be effectively locked without significant coherence leakage.

How low should the RF field strength be in order to selectively create the two-spin central DQ transition? The rotary resonance recoupling experiments require that the effective RF field matches the spinning speed. One can easily see the conflict, since on the one hand we want to spin faster than the residual second-order quadrupolar broadening (>20 kHz), but on the other hand we must use low RF irradiation to avoid adiabatic passage transfers. To answer this question it is useful to investigate how the adiabatic transfer depends on orientation namely to analyze all possible orientations of the quadrupolar interaction. Fig. 7 shows how each orientation of the quadrupolar interaction contributes to the MAS lineshape. In (a) all orientations possible are displayed on a sphere (each orientation of the quadrupolar tensor in the principal axis system corresponds to the α, β and γ angles of that point) and they are colour coded as a function of, where they contribute to the MAS lineshape shown in (b). We can simulate what happens with one spin $I = 5/2$ nucleus during the spin lock pulse sequence shown in Fig. 4a. In

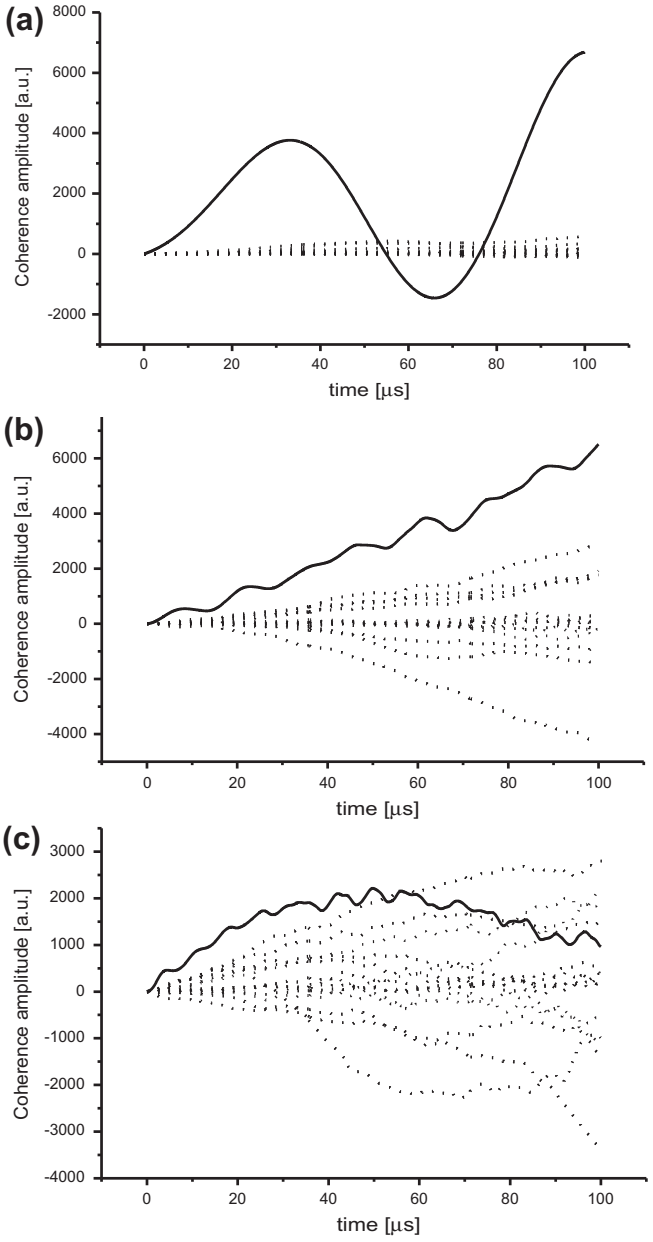

Fig. 5. Excitation profile for the 25 DQ coherences, spin locking RF power was (a) 5 kHz, (b) 25 kHz and (c) 50 kHz. Excitation profile for the central DQ transition is drawn with solid line. A spin system formed by two identical spin $I = 5/2$ nuclei ($C_{qcc} = 4$ MHz $\eta = 0.4$) was considered. The equilibrium density matrix of the spin system was evolved under the first-order quadrupolar Hamiltonian, spin lock irradiation Hamiltonian and a 200 Hz isotropic coupling Hamiltonian. The spin system was spun at $\nu_{MAS} = 10$ kHz.

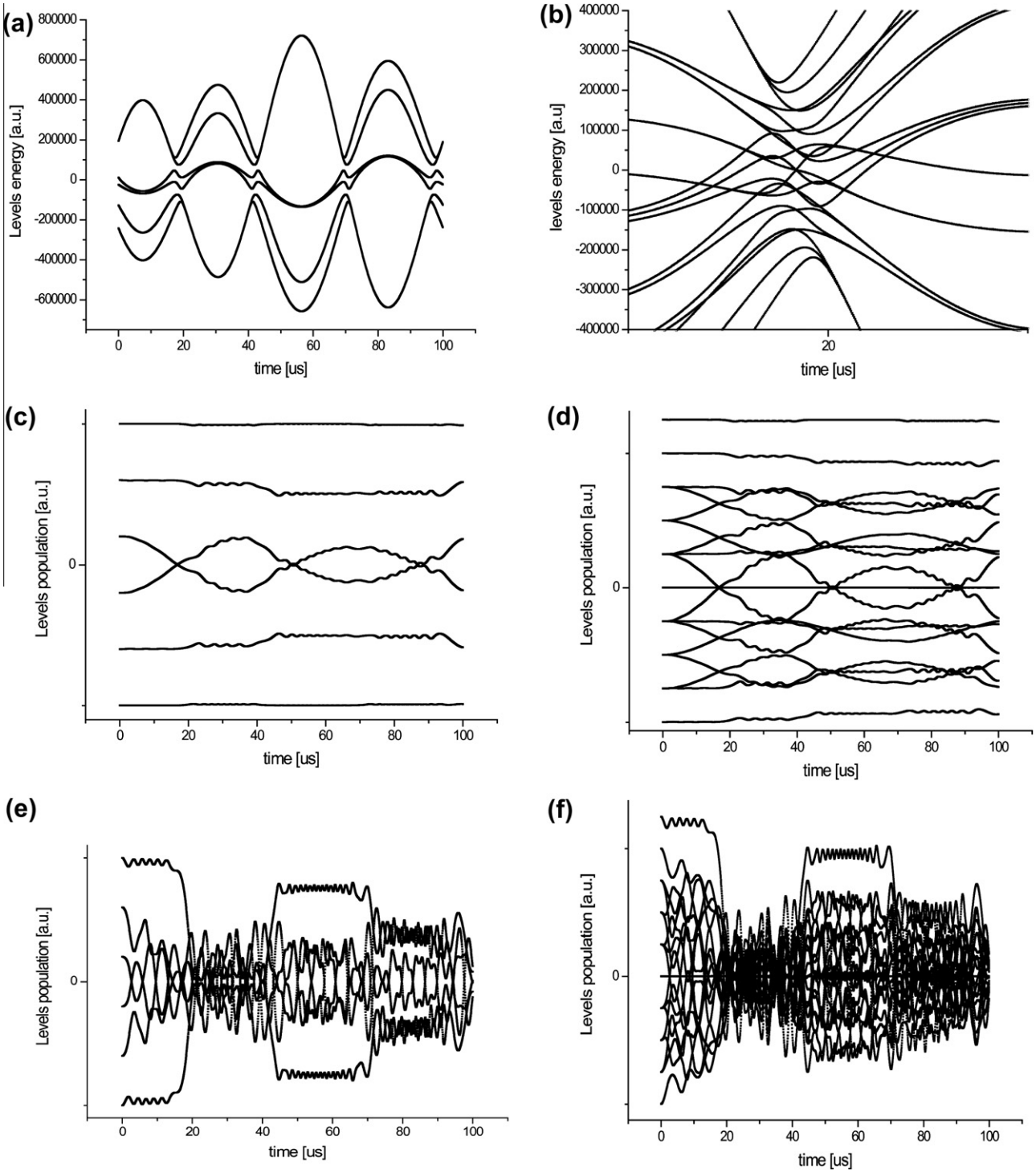

Fig. 6. Variation of the energy levels during one rotor period (ν_{MAS} = 10 kHz) for (a) a spin I = 5/2 nucleus (C_{qcc} = 4 MHz and η = 0.4) and (b) two coupled spin I = 5/2 nuclei (both with C_{qcc} = 4 MHz and η = 0.4). Evolution of energy level population for one orientation (α = 156, β = 98, γ = 12) during one rotor period for a spin I = 5/2 nucleus (c and d) and for two coupled spin I = 5/2 nuclei (e and f). ν_{RF} = 5 kHz (for c and d); ν_{RF} = 50 kHz (for e and f). Only the effect o the first-order quadrupolar Hamiltonian was considered.

Fig. 8, we monitor the changes that occur in the population of the |3/2> energy level of a single spin I = 5/2 nucleus. In this figure a light colour means that orientation is not much affected whereas a dark colour means that orientation is very strongly affected and many adiabatic passage transfers occur during one rotor period. Fig. 8a shows that for 2 kHz RF irradiation most orientations are not significantly affected, and Fig. 8c shows that for 8 kHz most orientations are strongly affected. An intermediate RF field strength (4 kHz) produces an intermediate situation where some orientations are less affected that others but overall one can easily expect that such an irradiation implies significant losses in the central transition coherence.

In order to increase the RF field strength during homonuclear experiments on half-integer quadrupolar nuclei we propose a new sequence which consists in a normal rotary resonance irradiation but the amplitude is reduced for four short time periods

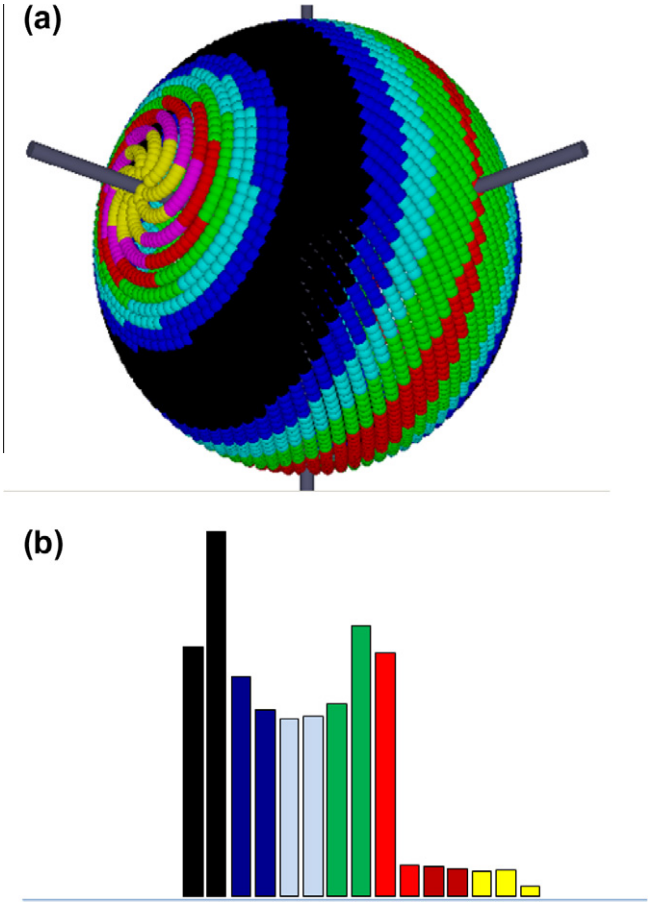

Fig. 7. (a) Contribution of different orientations of the quadrupolar tensor to the second-order quadrupolar MAS spectrum. (b) Central transition second-order quadrupolar MAS spectrum of a spin $I = 5/2$ nucleus ($C_{qcc} = 4$ MHz and $\eta = 0.1$).

during a rotor period. The pulse sequence used on the spin lock experiment is shown in Fig. 4b. The aim of reducing the amplitude is to avoid the adiabatic passage transfer that occurs during quadrupolar interaction zero crossings. For most orientations there are four zero crossings during one rotor period but the time they occur is different for each orientation. Therefore when optimizing such a pulse sequence one must look again at what happens to all orientations and for a quantitative analysis we monitored the changes that occur within the population of the |3/2> energy level of a spin $I = 5/2$ nucleus during spinning. Fig. 9a shows these changes during a normal spin lock experiment with the RF field strength of 4 kHz (similar with Fig. 8b). Fig. 9b shows the same changes during a spin lock experiment shown in Fig. 4b where the amplitude of the spin lock is reduced four times per rotor period. The same colour code as in Fig. 8 is used. One can clearly see that for the oR^3 sequence there are fewer changes in the |3/2> level population implying that adiabatic passage transfers are reduced.

3. Experimental details and discussions

For testing the oR^3 sequence in the DQ–SQ homonuclear correlation experiment we use the pulse sequence shown in Fig. 4c and d. It consists of R^3 (oR^3) spin lock pulses sandwiched between two soft 90° pulses to create the DQ coherence. The effective RF field strength of the spin lock pulses (R^3 or oR^3) matches the spinning speed while their duration equals a rotor period. Several spin lock pulses with y–y phase alternation can be applied. In this way both single spin DQ coherences and two-spin DQ coherences are created.

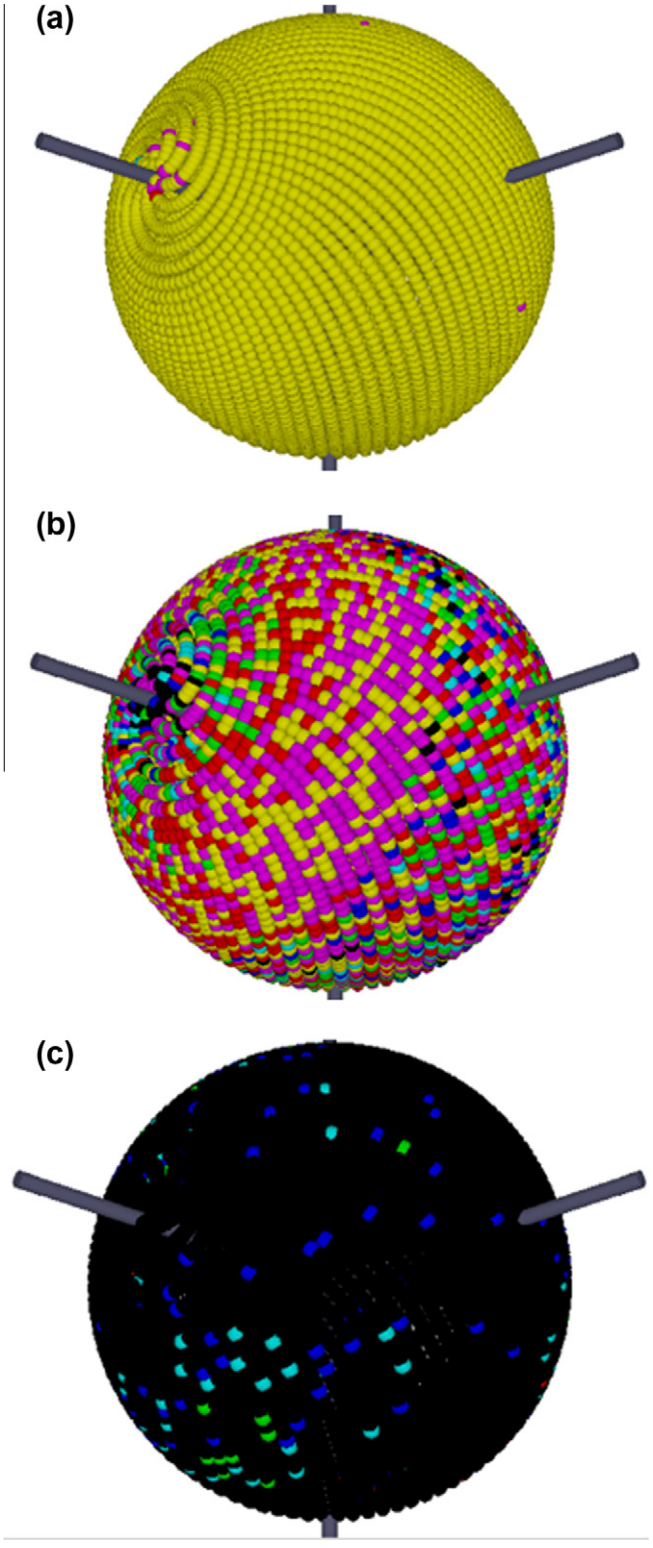

Fig. 8. Behaviour of spins with different orientations of first-order quadrupolar tensor during spin locking and MAS. All changes in the 3/2 level population during spin locking and MAS are added up. More changes imply more adiabatic passage transfers occur and therefore more likely that unwanted coherences appear. The figures are colour coded darker the colour more affected that orientation is ($\nu_{MAS} = 12$ kHz, (a) $\nu_{RF} = 2$ kHz, (b) $\nu_{RF} = 4$ kHz and (c) $\nu_{RF} = 8$ kHz). (For interpretation of the references to colour in this figure legend, the reader is referred to the web version of this article.)

A selective π pulse which was introduced by Kwack and Gan [25] for the STMAS experiment and later used by Mali et all [17] in the

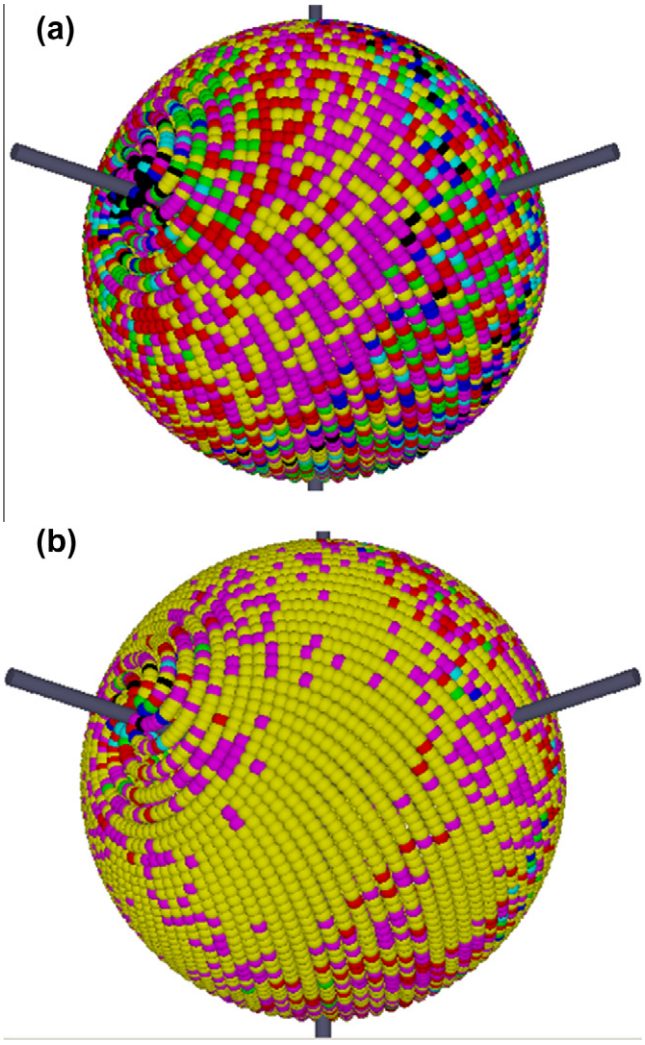

Fig. 9. Comparison between the effect of spin locking using R^3 (a) or oR^3 and (b) $\nu_{RF} = 4$ kHz; $\nu_{MAS} = 12$ kHz. The figures are colour coded darker the colour more affected that orientation is. The same conditions as for Fig. 8 apply. (For interpretation of the references to colour in this figure legend, the reader is referred to the web version of this article.)

DQ–SQ correlation experiments can be used to distinguish between single spin DQ coherences and two-spin DQ coherences. A two-spin DQ coherence for example $S_+^{3-4}I_+^{3-4}$ remains a DQ coherence after such a pulse, $S_-^{3-4}I_-^{3-4}$, whereas a single spin DQ coherence for example $S_+^{1-2}S_+^{3-4}I_z$ is converted to a single spin zero-quantum coherence $S_+^{1-2}S_-^{3-4}I_z$. Here S and I represents the two ^{27}Al spins involved and S^{1-2}, S^{3-4} refers to the fictitious spin ½ operators (introduced by Vega [26]) for a satellite transition and central transition respectively. The remaining two-spin DQ coherences are evolved for the t1 time and then converted to a ZQ coherence again by R^3 (oR^3) spin lock pulses sandwiched between two soft 90° pulses. A Z-filter converts the remaining ZQ coherences into a detectable SQ signal. The coherence pathway of the DQ–SQ correlation experiment is shown in Fig. 4e.

We chose as model samples, YAG and γAl_2O_3 (commercial γAl_2O_3 99.5% (metals based) from Johnson and Mattey GmbH). In both samples ^{27}Al occupy a tetrahedral and an octahedral position. Fig. 10 shows the ^{27}Al MAS spectra of the two samples, span at 20 kHz (YAG) and 12 kHz (γAl_2O_3) respectively. For YAG [27] the two tetrahedral and octahedral peaks are at 77.24 ppm and 5.71 ppm respectively whereas for γAl_2O_3 the two tetrahedral and octahedral peaks are at 73.8 ppm and 13.8 ppm respectively.

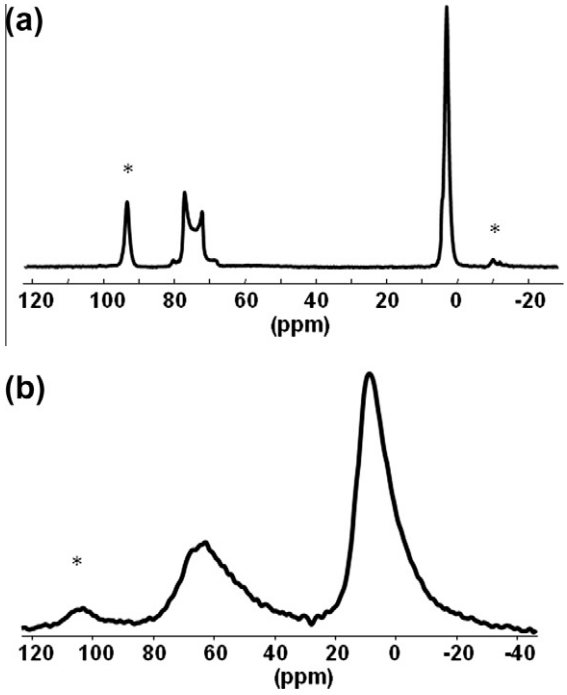

Fig. 10. ^{27}Al MAS spectra of (a) YAG $\nu_{MAS} = 20$ kHz and (b) γAl_2O_3 $\nu_{MAS} = 12$ kHz. The stars indicate spinning sidebands.

The normal MAS spectra indicate some distribution of the NMR parameters for γAl_2O_3.

Fig. 11 shows the first slice from a 2D DQ–SQ correlation experiment performed on ^{27}Al on YAG The experiment (pulse sequence shown in Fig. 4c and 4d) was performed using oR^3 (Fig. 11a) and R^3 (Fig. 11b) recoupling sequences respectively. The YAG sample was spun at 12 kHz and different effective RF field strengths (from 11 kHz to 13.5 kHz) were used during the recoupling sequence. oR^3 sequence clearly performs better for the tetrahedral site with bigger quadrupolar coupling constant.

Fig. 12a shows the DQ–SQ homonuclear correlations for YAG measured at 20 kHz spinning speed. The measurement was performed using a Bruker 850 MHz (^{27}Al $\omega_L = 221.55$ MHz) Avance III spectrometer using a Bruker 2.5 mm HX probe. 256 scans were acquired for 64 t_1 increments using 2 s relaxation delay (i.e. experiment time of 9 h). The effective RF power for the 90° pulse and conversion filter was set to about 17 kHz effective RF field strength giving a 14 μs 90° pulse. An effective RF irradiation of 10 kHz was applied for the oR^3 sequence. In Fig. 12b is shown the DQ–SQ homonuclear correlations of γAl_2O_3 measured at 12 kHz spinning speed using a Bruker 500 MHz (^{27}Al $\omega_L = 130.31$ MHz). Advance III spectrometer using a Bruker 4 mm HX probe. 1280 scans with a d1 of 0.2 s were acquired for 160 t_1 transients (i.e. experimental time of 11 h). The effective RF power for the 90° pulse and conversion filter was set to about 16.6 kHz giving a 15 μs 90° pulse. An effective RF irradiation of 12 kHz was applied for the oR^3 sequence.

YAG has a cubic crystal structure with ^{27}Al in a octahedral ($^{27}Al_1$) and tetrahedral ($^{27}Al_2$) positions. In a second sphere of coordination each $^{27}Al_1$ sees six $^{27}Al_2$ at 3.35 Å distance and eight $^{27}Al_1$ at a distance of 5.19 Å. Each $^{27}Al_2$ sees four $^{27}Al_1$ at 3.35 Å and four Al_2 at 3.6 Å [28]. The distances are to be considerate only approximate as there are quite some variations in literature. These ^{27}Al pairs are forming a two spin system where the DQ coherences are generated. There are three types of ^{27}Al pairs: $^{27}Al_1$–$^{27}Al_1$ pair, $^{27}Al_1$–$^{27}Al_2$ pair, and $^{27}Al_2$–$^{27}Al_2$ pair. Their DQ coherences appear at 11 ppm, 83 ppm and 156 ppm respectively, see Fig. 12a.

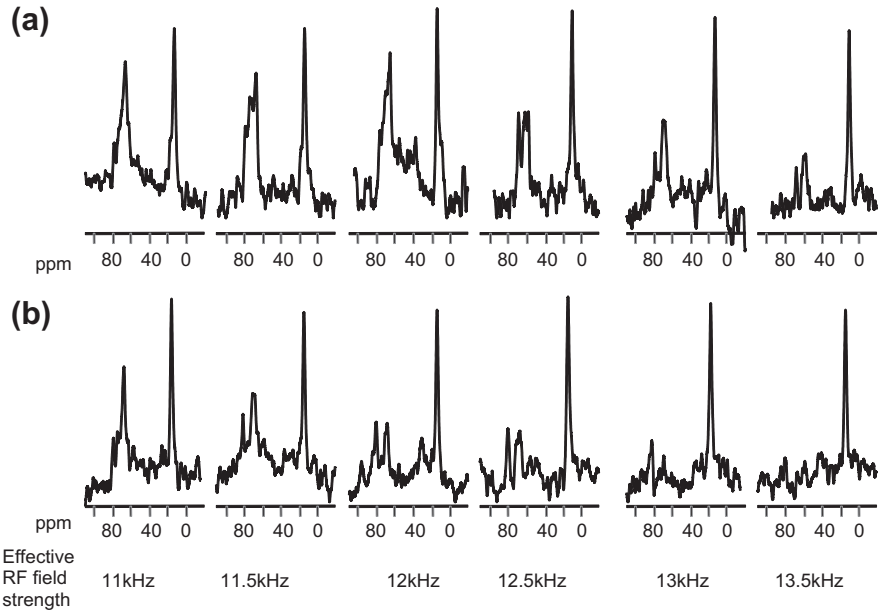

Fig. 11. First sliced spectrum from a 2D DQ–SQ homonuclear correlation experiment obtained for different effective RF field strengths (a) spectra obtained using oR^3 (pulse sequence shown in Fig. 4d.) and (b) spectra obtained using R^3 (pulse sequence shown in Fig. 4c). ν_{MAS} = 12 kHz.

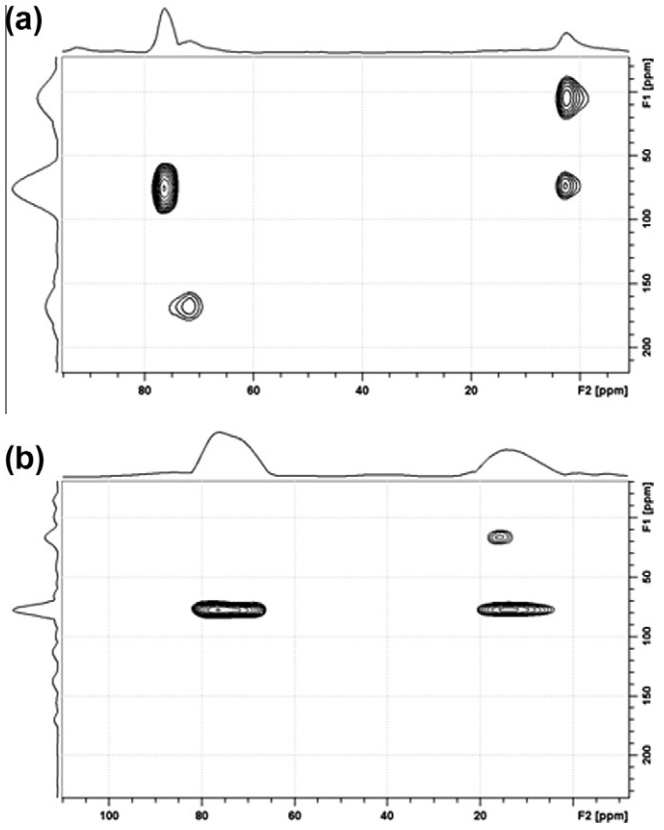

Fig. 12. ^{27}Al–^{27}Al DQ–SQ homonuclear correlation spectra (a) YAG ν_{MAS} = 20 kHz and (b) γAl_2O_3 ν_{MAS} = 12 kHz.

The second sample investigated using the DQ–SQ homonuclear correlation experiment shown on Fig. 4d was γAl_2O_3. Despite the widespread use of γAl_2O_3 the structure and the composition is still under debate [29]. X-ray diffraction suggests a spinel structure with 24 cations and 32 anions per unit cell. However to satisfy the stoichiometry some cation sites need to be vacant. The distribution of the vacancies is still under debate. The structure is formed from a layer containing both octahedral aluminium ($^{27}Al_1$) and oxygen and another layer containing both octahedral ($^{27}Al_1$) and tetrahedral aluminium ($^{27}Al_2$) and oxygen [14]. In this case the X-ray structure shows six $^{27}Al_1$–$^{27}Al_1$ pairs with 2.8 Å internuclear distance, six $^{27}Al_1$–$^{27}Al_2$ pairs with 3.3 Å internuclear distance, and four $^{27}Al_2$–$^{27}Al_2$ pairs with 3.5 Å internuclear distance (again due to large variation of these values in literature the distances are approximate and given only as a guidance). The DQ–SQ correlation spectrum shown in Fig. 12b reveals that double quantum coherence peaks appears for two coupled octahedral ^{27}Al (at 26 ppm) and for an octahedral ^{27}Al coupled with a tetrahedral ^{27}Al sites (at 86 ppm). There is no peak for two coupled tetrahedral ^{27}Al and this indicates that the vacancies mainly occur among these sites.

4. Conclusions

The paper presents a numerical investigation of a spin system formed by two spin $I = 5/2$ nuclei. It demonstrates that the first-order quadrupolar interactions of the two spins involved can compensate each other. The compensation is complete for identical spins resulting in DQ transitions free of first-order quadrupolar broadening. It is shown that such DQ coherences can have significant intensity and since they cannot be removed by phase-cycling they can broaden the experimental spectrum and lower the intensity of the desired CT DQ coherence. This can be avoided if selective (low) RF irradiation is used. The paper introduces the optimized rotary resonance recoupling sequence which allows for larger RF amplitude without exciting undesired DQ coherences. The oR^3 sequence is used to measure the DQ–SQ homonuclear correlation spectra of YAG and γAl_2O_3. The homonuclear correlation spectrum of gamma alumina is used to conclude that the vacancies in the structure mainly occur on the tetrahedral aluminium sites.

Acknowledgment

The UK 850 MHz solid-state NMR Facility used in this research was funded by EPSRC and BBSRC, as well as the University of

Warwick including via part funding through Birmingham Science City Advanced Materials Project supported by Advantage West Midlands (AWM) and the European Regional Development Fund (ERDF). Jeremy Titman is acknowledged for guidance in elaborating the manuscript. I thank Z. Gan for inspiring discussions.

Appendix A. Supplementary material

Supplementary data associated with this article can be found, in the online version, at doi:10.1016/j.jmr.2010.11.007.

References

[1] L. Frydman, J.S. Hardwood, Isotropic spectra of half-integer quadrupolar spins from bidimensional magic-angle-spinning NMR, J. Am. Chem. Soc. 117 (1995) 5367–5369.
[2] Z. Gan, Isotropic NMR spectra of half-integer quadrupolar nuclei using satellite transitions and magic-angle spinning, J. Am. Chem. Soc. 122 (2000) 3242–3243.
[3] S.E. Ashbrook, Recent advances in solid-state NMR spectroscopy of quadrupolar nuclei, Phys. Chem. Chem. Phys. 11 (2009) 6892–6905.
[4] S.E. Ashbrook, M.J. Duer, Structural information from quadrupolar nuclei in solid state NMR, Concepts Magn. Reson. A 28 (2006) 183–248.
[5] M.H. Levitt, in: D.M. Grant, R.K. Harris (Eds.), Encyclopedia of Nuclear Magnetic Resonance: Supplementary Volume, Wiley, Chichester, England, 2002, pp. 165–196.
[6] M.H. Frey, S.J. Opella, High-resolution features of the C13 NMR spectra of solid amino-acids and peptides, JCS Chem. Commun. (1980) 474–475.
[7] E.M. Menger, W.S. Veeman, Quadrupole effects in high-resolution P-31 solid state NMR spectra of triphenylphosphine copper(I), J. Magn. Reson. 46 (1982) 257–268.
[8] A.J. Painter, M.J. Duer, Double-quantum-filtered nuclear magnetic resonance spectroscopy applied to quadrupolar nuclei in solids, J. Chem. Phys. 116 (2002) 710–722.
[9] D. Massiot, F. Fayon, B. Alonso, J. Trebosc, J.P. Amoreux, Chemical bonding differences evidenced from J-coupling in solid state NMR experiments involving quadrupolar nuclei, J. Magn. Reson. 164 (2003) 160–164.
[10] D. Iuga, C. Morais, Z.H. Gan, D.R. Neuville, L. Cormier, D. Massiot, NMR heteronuclear correlation between quadrupolar nuclei in solids, J. Am. Chem. Soc. 127 (2005) 11540–11541.
[11] H.T. Kwak, P. Srinivasan, J. Quine, D. Massiot, Z. Gan, Satellite transition rotational resonance of homonuclear quadrupolar spins: magic-angle effect on spin-echo decay and inversion recovery, Chem. Phys. Lett. 376 (2003) 75–82.
[12] M. Baldus, D. Rovnyak, R.G. Griffin, Radio-frequency-mediated dipolar recoupling among half-integer quadrupolar spins, J. Chem. Phys 112 (2000) 5902–5909.
[13] T.G. Ajithkumar, A.P.M. Kentgens, Homonuclear correlation experiments of half-integer quadrupolar nuclei using multiple-quantum techniques spinning at a P-4 magic angle, J. Am. Chem. Soc. 125 (2003) 2398–2399.
[14] I. Hung, A.P. Howes, B.G. Parkinson, T. Anupold, A. Samoson, S.P. Brown, P.F. Harrison, D. Holland, R. Dupree, Determination of the bond-angle distribution in vitreous B2O3 by B-11 double rotation (DOR) NMR spectroscopy, J. Solid Sate Chem. 182 (2009) 2402–2408.
[15] S. Wi, J.W. Logan, D. Sakellariou, J.D. Walls, A. Pines, Rotary resonance recoupling for half-integer quadrupolar nuclei in solid-state nuclear magnetic resonance spectroscopy, J. Chem. Phys. 117 (2002) 7024–7033.
[16] M. Eden, H. Annersten, A. Zazzi, Pulse-assisted homonuclear dipolar recoupling of half-integer quadrupolar spins in magic-angle spinning NMR, Chem. Phys. Lett. 410 (2005) 24–30.
[17] G. Mali, G. Fink, F. Taulelle, Detecting proximities between quadrupolar nuclei by double-quantum NMR, J. Chem. Phys. 120 (2004) 11726–11744.
[18] M. Eden, D. Zhou, J.H. Yu, Improved double-quantum NMR correlation spectroscopy of dipolar-coupled quadrupolar spins, J. Chem. Phys. Lett. 431 (2006) 397–403.
[19] M. Eden, Homonuclear dipolar recoupling of half-integer spin quadrupolar nuclei: techniques and applications, Solid State Nuc. Magn. Reson. 36 (2009) 1–10.
[20] A. Brinkmann, A.P.M. Kentgens, T. Anupold, S. Samoson, Symmetry-based recoupling in double-rotation NMR spectroscopy, J. Chem. Phys. 129 (2008) 174507.
[21] A.J. Vega, MAS NMR spin locking of half integer quadrupolar nuclei, J. Magn. Reson. 96 (1992) 50–68.
[22] G. Oas, R.G. Griffin, M.H. Levitt, Rotary resonance recoupling of dipolar interactions in magic-angle-spinning NMR spectroscopy, J. Chem. Phys 89 (1988) 692.
[23] Q. Wang, B. Hu, O. Lafon, J. Trébosc, F. Deng, J.P. Amoureux, Double-quantum homonuclear NMR correlation spectroscopy of quadrupolar nuclei subjected to magic-angle spinning and high magnetic field, J. Magn. Reson. 200 (2) (2009) 251–260.
[24] S.E. Ashbrook, S. Wimperis, Spin-locking of half-integer quadrupolar nuclei in nuclear magnetic resonance of solids: second-order quadrupolar and resonance offset effects, J. Chem. Phys. 131 (2009) 194509.
[25] H.T. Kwak, Z.H. Gan, Double quantum filtered STMAS, J. Magn. Reson. 164 (2) (2003) 369–372.
[26] S. Vega, Y.J. Naor, Triple quantum NMR on spin systems with $I = 3/2$ in solids, J. Chem. Phys. 75 (1981) 75–86.
[27] D. Massiot, C. Bessada, J.P. Coutures, F. Taulelle, A quantitative study of aluminium-27 MAS NMR in crystalline YAG, J. Magn. Reson. 90 (2) (1990) 231–242.
[28] L. Dobrzycki, E. Bulska, D.A. Pawlak, Z. Frukacz, Wozniak, structure of YAG crystals doped/substituted with erbium and ytterbium, Inorg. Chem. 43 (2004) 7656–7664.
[29] K. Solhberg, S.J. Pennycook, S.T. Pantelides, Explanation of the observed dearth of three-coordinated Al on gamma-alumina surfaces, J. Am. Chem. Soc. 121 (1999) 7493–7499.